

# Chapter 4

## Structure and Phase Behaviour of DLPE–Cholesterol Membranes

### 4.1 Introduction

In chapter 3, we described a novel modulated ( $P_\beta$ ) phase induced by cholesterol in DPPC and DMPC. The structure of this phase is somewhat similar to that of the ripple ( $P_{\beta'}$ ) phase seen in some phosphatidylcholines in between the main- and pre-transitions. It is known that the ripple phase occurs only in lipids that have a non-zero chain tilt in the gel phase. As discussed in the previous chapter, the  $P_\beta$  phase does not have an average chain tilt. Therefore, it is interesting to check whether it also exists in binary mixtures of cholesterol with lipids that have no chain tilt in the gel phase. This motivated us to study mixtures of phosphatidylethanolamine (PE) and cholesterol, as PEs are known to exhibit a gel phase having zero tilt of the hydrocarbon chains. We have chosen dilauroyl phosphatidylethanolamine (DLPE) due to the appropriate temperature range of its gel phase, which is easily accessible with our experimental setup.

This chapter deals with the structure and phase behaviour of DLPE-cholesterol mixtures. Before we discuss our experimental results, we summarize earlier studies on PE–cholesterol mixtures in section 4.2. Although PEs and PE–cholesterol mixtures exhibit non lamellar phases at high temperatures, we will be concentrating on the lamellar phases that occur at lower temperatures. Our experimental results on DLPE–cholesterol mixtures will be described in section 4.3. An electron density profile of DLPE–cholesterol bilayers has been

deduced from the diffraction data and is presented in section 4.4. Finally we discuss our results in section 4.5.

## 4.2 Earlier studies

Besides phosphatidylcholines (PCs), phosphatidylethanolamines (PEs) are the most common phospholipids found in plasma membranes. PEs differ from PCs in the structure of their head group (see chapter 1, section 1.2). Unlike PCs, PEs can form intermolecular hydrogen bonds between the head groups. Interaction of cholesterol with PEs is known to be weaker than that with PCs [1]. There have been a large number of studies, using a variety of experimental techniques, on the influence of cholesterol on PE bilayers [2, 3, 4, 5, 6, 7, 8, 9, 10]. One interesting feature reported in PE–cholesterol mixtures concerns the formation of the  $L_c$  phase. In general, the highly ordered  $L_c$  phase nucleates only after long incubation at low temperatures, typically 4°C. The presence of cholesterol in PE bilayers facilitates the formation of the  $L_c$  phase [2, 7]. Once formed, the  $L_c$  phase transforms into  $L_\alpha$  only at a temperature much above the  $L_\beta \rightarrow L_\alpha$  transition temperature [2]. Studies of the influence of cholesterol on the thermotropic phase behaviour of a homologous series of linear saturated PEs by McMullen et al. found that dimyristoyl phosphatidylethanolamine (DMPE), dipalmitoyl phosphatidylethanolamine (DPPE) and distearoyl phosphatidylethanolamine (DSPE) do not exhibit the  $L_c$  phase in the absence of cholesterol under their experimental conditions [2]. Differential scanning calorimetry (DSC) thermograms of PE–cholesterol mixtures show a single transition peak at cholesterol concentrations ( $X_c$ ) < 30 mol%. However, for  $X_c > 30$  mol%, two transition peaks appear on heating. These peaks correspond to  $L_c \rightarrow L_\beta$  and  $L_\beta \rightarrow L_\alpha$  transitions (Fig. 4.1). Progressive decrease of transition temperature, enthalpy, and increase in the width of the thermogram with increasing  $X_c$ , for  $X_c < 30$  mol%, is similar to that observed in PC–cholesterol mixtures. However, due to the formation of the  $L_c$  phase at  $X_c > 30$  mol%, the transition temperature and enthalpy increase with increasing  $X_c$  during heating cycle. These mixtures show a single  $L_\alpha \rightarrow L_\beta$  transition upon cooling from high temperatures, indicating that once the  $L_c$  phase melts, it does not reappear immediately on

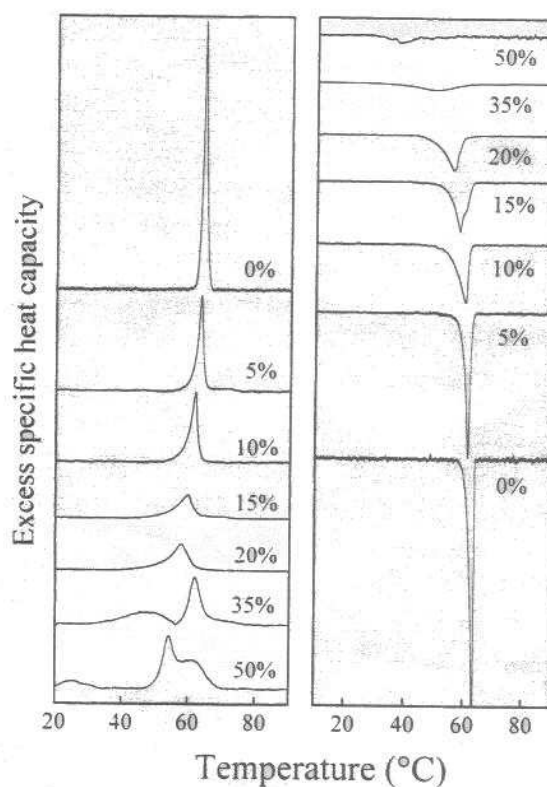


Figure 4.1: DSC thermograms of DPPE–cholesterol mixtures at various cholesterol concentrations as indicated by the labels on the curves, obtained during heating (left) and cooling (right). [2].

cooling.

$^2\text{H}$  NMR and infrared (IR) spectroscopy studies by Paře et al. [11] found that cholesterol makes POPE bilayer more disordered below  $T_m$  and more ordered above  $T_m$ , as in the case of PC-cholesterol mixtures. At higher  $X_c$  ( $> 30$  mol%), NMR spectra suggest axially symmetric motion of the chains as in the case of the fluid phase, but the average hydrocarbon chain order parameter ( $S$ ) was found to be higher than that in the fluid phase of PEs without cholesterol. Typical value of  $S$  is  $\sim 0.3$  for  $X_c = 45$  mol% at  $32^\circ\text{C}$ , whereas that of pure lipid is  $\sim 0.2$ . Results of DSC, NMR, IR spectroscopy studies taken together suggest that there is a two-phase region below the chain melting transition temperature ( $T_m$ ) at  $10 < X_c < 30$ . They are believed to be the gel ( $L_\beta$ ) phase and a cholesterol-rich fluid ( $l_o$ ) phase. A partial phase diagram proposed based on IR and NMR studies is shown in Fig. 4.2. X-ray diffraction studies on PE–cholesterol mixtures have also revealed two sets of lamellar

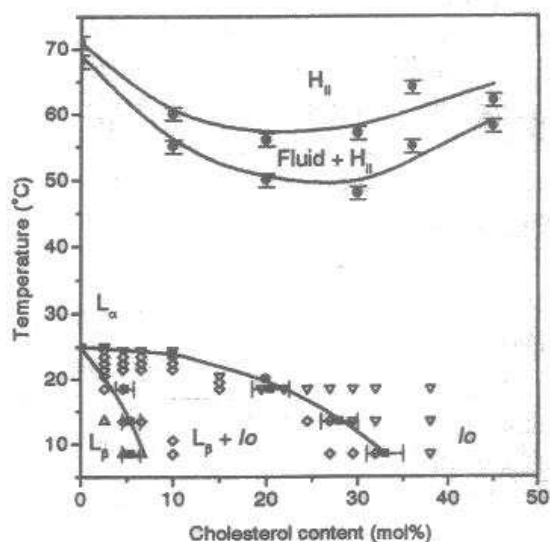


Figure 4.2: A partial phase diagram of POPE–cholesterol mixtures obtained from IR and NMR spectroscopy.  $H_{II}$  : inverted hexagonal phase,  $L_{\alpha}$  : fluid phase,  $L_{\beta}$  : gel phase,  $l_o$  : cholesterol–rich fluid phase [11].

reflections, similar to those of gel and fluid phases for  $10 < X_c < 30$  [3, 5, 11]. At  $X_c > 30$  mol%, the cholesterol–rich  $l_o$  phase was found as in the case of PC–cholesterol mixtures. It is important to note that there is no evidence for the coexistence of two fluid phases above  $T_m$  as found in PC–cholesterol mixtures [12]. However, many unsaturated PEs undergo a transition from a lamellar to a nonlamellar phase at high temperatures (much above  $T_m$ ) [3, 5, 11]. It is interesting to note that cholesterol promotes a cubic phase at intermediate  $X_c$  (5–20 mol%) instead of the inverted hexagonal phase found in its absence. The formation of such nonlamellar phases have an important role in the pathways of many cellular events [13].

### 4.3 Experimental results

Experiments on DLPE–cholesterol mixtures have been carried out in order to compare their phase behaviour with that of DPPC–cholesterol mixtures. Samples with  $X_c$  of 0, 2.5, 5, 7.5, 10, 15, 20 and 30 mol% were studied. All experiments were done with oriented samples at  $98 \pm 2\%$  relative humidity (RH), as described in chapter 2. DLPE bilayers, at high hydration,

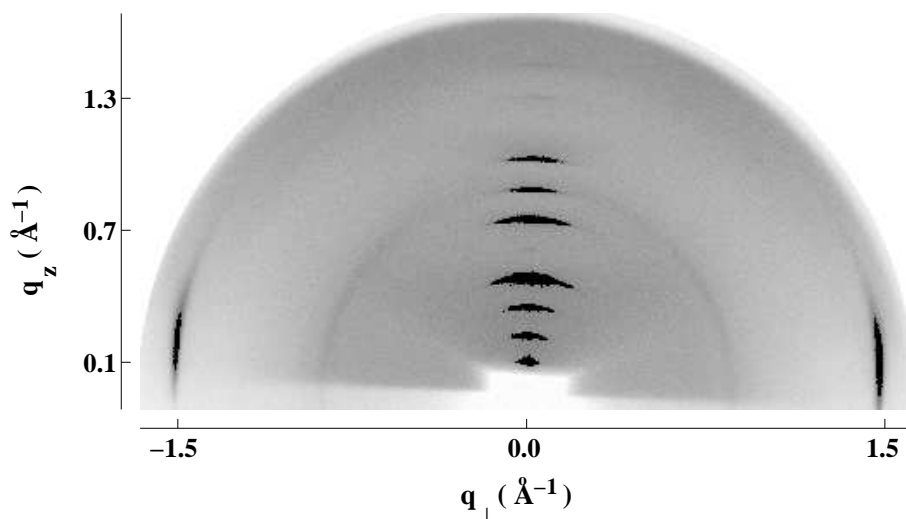


Figure 4.3: Diffraction pattern of the  $L_\beta$  phase of DLPE ( $T = 10^\circ\text{C}$ ,  $\text{RH} = 98\%$ ). The absence of chain tilt is indicated by the on-axis ( $q_z = 0$ ) wide angle reflections. The shadow at the bottom is due to absorption by the substrate. The diffuse ring near  $q = 0.7$  is due to the mylar windows of the sample chamber.

exhibit the fluid ( $L_\alpha$ ) phase above  $T_m$  ( $\sim 30^\circ\text{C}$ ) and the gel ( $L_\beta$ ) phase below  $T_m$  [14]. A typical diffraction pattern of the gel phase is shown in Fig. 4.3. Wide angle reflections at  $q_z = 0$  indicate that there is no tilt of the hydrocarbon chains with respect to the bilayer normal.

Incorporation of cholesterol into DLPE bilayers facilitates the formation of a highly ordered phase (Fig. 4.4), which transforms at around  $45^\circ\text{C}$  into the  $L_\alpha$  phase. A similar phase is also seen in pure DLPE after long incubation at low temperature ( $\sim 4^\circ\text{C}$ ), as shown in Fig. 4.5. On cooling, the  $L_\alpha$  phase continues down to  $30^\circ\text{C}$ , at which temperature the  $L_\beta$  phase is formed. We have not observed the highly ordered phase on cooling, even at the lowest temperature studied ( $5^\circ\text{C}$ ). However, it was formed on incubating the sample at  $4^\circ\text{C}$  for a few hours; the presence of cholesterol seems to make this transformation faster, as reported earlier by McMullen et al. [2]. This phase appears at  $\sim 10^\circ\text{C}$  on cooling when the samples were not kept at high temperatures (above  $T_m$ ) for a sufficiently long time (typically 1 hour) (Fig. 4.6)

For  $2.5 \leq X_c < 10$  mol%, we have observed two sets of lamellar reflections; one of them has spacing similar to that of the gel phase and other one is similar to the fluid phase of pure DLPE (Fig. 4.7). This observation is in agreement with the previous report by Takahashi et

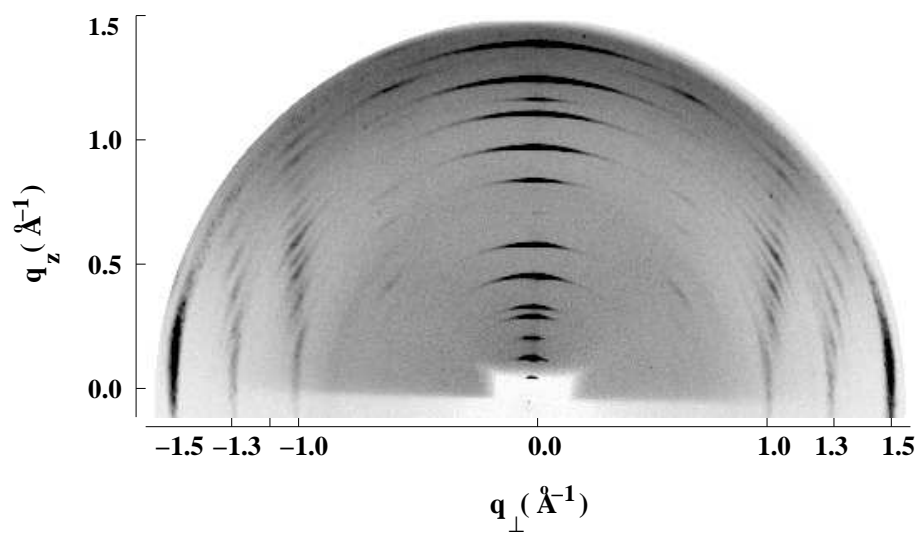


Figure 4.4: Diffraction pattern of a highly ordered phase of DLPE-cholesterol mixtures observed in a sample before heating to high temperatures ( $X_c = 10$  mol% ).

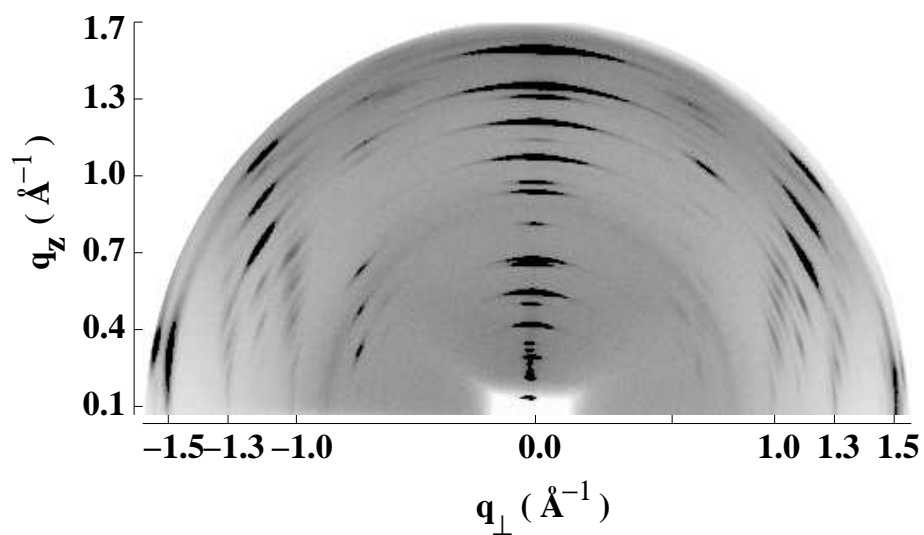


Figure 4.5: Diffraction pattern of a highly ordered phase of DLPE before heating to high temperatures.

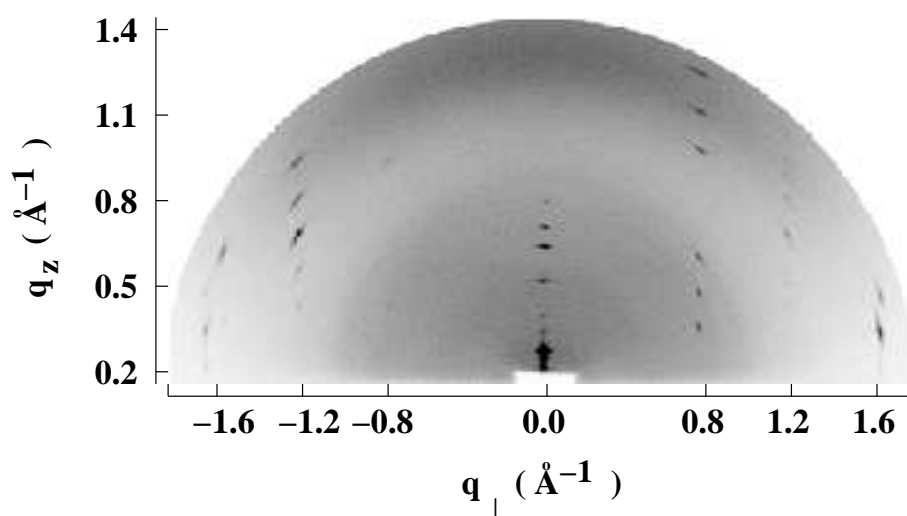


Figure 4.6: Diffraction pattern of a highly ordered phase of DLPE-cholesterol mixtures observed on cooling the sample from the  $L_\alpha$  phase.

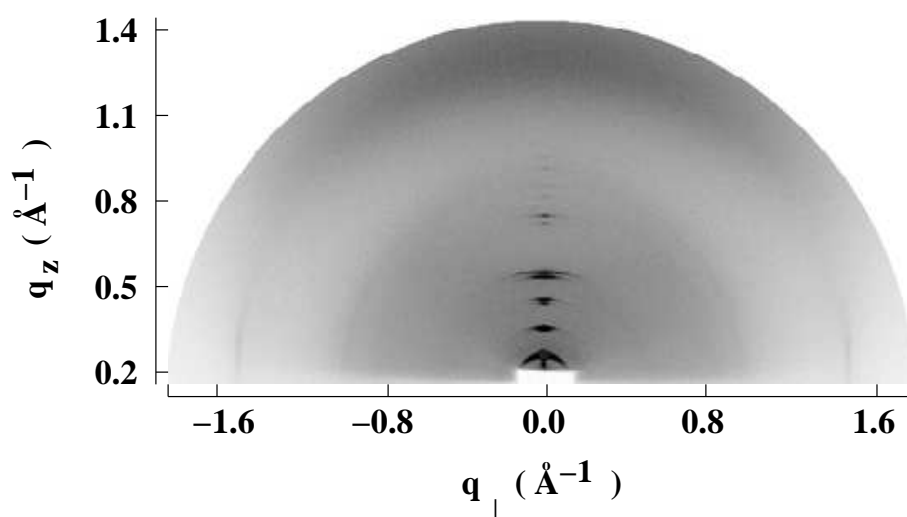


Figure 4.7: Diffraction pattern of a DLPE-cholesterol mixture showing the coexistence of the  $L_\beta$  and  $L_\alpha$  phases ( $X_c = 5$  mol%,  $T = 30^\circ\text{C}$ ,  $\text{RH} = 98\%$ ).

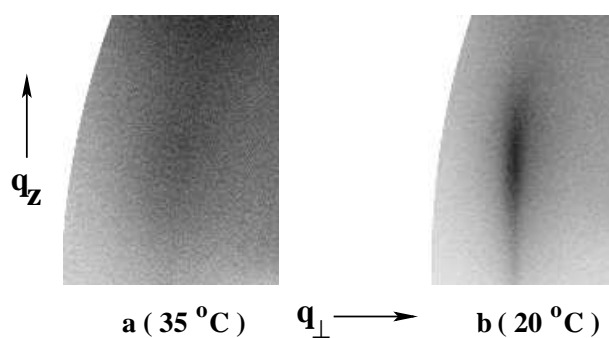


Figure 4.8: The wide angle reflections of DLPE-cholesterol mixture at  $X_c = 10$  mol% ( $d = 4.5 \text{ \AA}$  at  $35^\circ\text{C}$ ,  $d = 4.2 \text{ \AA}$  at  $20^\circ\text{C}$ ).

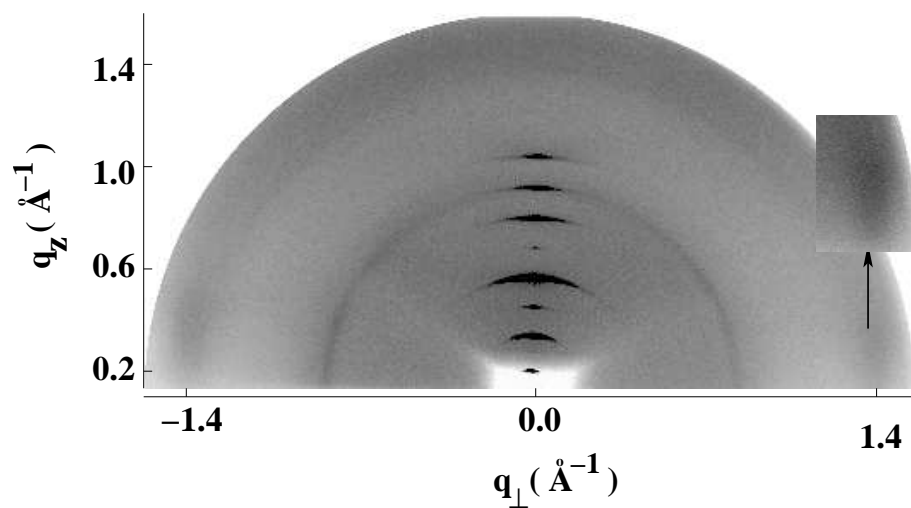


Figure 4.9: Diffraction pattern of the cholesterol-rich  $l_o$  phase ( $X_c = 20$  mol%,  $T = 10^\circ\text{C}$ ,  $\text{RH} = 98\%$ ). The inset is the wide angle reflection at a higher contrast. The diffuse ring near  $q = 0.7$  is due to the mylar windows of the sample chamber.

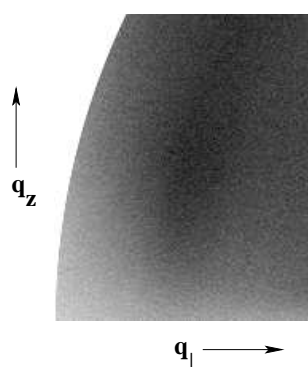


Figure 4.10: The wide angle reflection of DLPE-cholesterol mixture at  $X_c = 20$  mol% ( $T = 40^\circ\text{C}$ ,  $\text{RH} = 98\%$ ,  $d = 4.6$  Å).

Table 4.1: Lamellar spacings  $d$  (Å) of DLPE-cholesterol mixtures as a function of temperature (RH =  $98 \pm 2$  %). Two sets of spacings correspond to the coexistence of  $L_\alpha$  and  $L_\beta$  phases. The error in  $d$  is  $\pm 0.3$  Å.

T (°C)	$X_c$ (mol%)							
	0	2.5	5	7.5	10	15	20	30
45	43.6	43.1	43.3	43.3	44.0	45.5	45.8	46.2
40	43.6	44.1	43.5	43.4	44.7	46.6	46.1	46.7
35	44.1	44.6	44.1	44.5	45.2	47.1	46.4	46.8
30	48.1	45.2 ; 47.7	45.3 ; 47.5	45.6	45.8	47.4	47.1	46.8
25	48.4	47.8	47.8 ; 48.1	47.4 ; 48.7	47.6	48.1	48.1	46.8
20	48.9	48.6	48.2	48.4	47.9	49.1	48.3	47.8
15	49.3	48.6	48.4	48.4	48.3	49.1	48.4	47.8
10	49.5	48.6	48.4	48.4	47.9	49.3	48.4	47.8

al. [3]. At  $X_c = 10$  mol%, we have observed the diffuse wide angle reflection, condensed at  $q_z = 0$  at temperatures above  $T_m$  (Fig. 4.8 a). However, below  $T_m$ , the wide angle reflection becomes sharp, indicating fluid to gel transition, as shown in Fig. 4.8 b. At  $X_c > 10$ , we have observed a lamellar fluid ( $L_\alpha$ ) phase rich in cholesterol throughout the temperature range studied (Fig. 4.9). The wide angle reflection in the fluid ( $L_\alpha$ ) phase rich in cholesterol at  $X_c = 20$  mol% is shown in Fig. 4.10. The d-spacings of the different phases obtained from the diffraction data of DLPE–cholesterol mixtures are given in table 4.1. The spacing of the wide angle reflection increases from 4.2 Å to 4.6 Å as  $X_c$  is increased from 0 to 30 mol% at a given temperature. A similar trends was found with increasing temperature at a given  $X_c$ .

#### 4.4 Electron density profile of the $l_o$ phase

We have constructed the transbilayer electron density profile from the diffraction data (Fig. 4.11). Procedure for calculating the electron density profile has been described in chapter 2. In order to phase the reflections we have used a three delta function and Gaussian models, as discussed in chapter 2. We fit the corrected experimental intensity with that obtained from model using a standard Levenberg Merquardt technique for non linear least squares fitting. Phases were obtained from the best fit. The calculated structure factors and the model

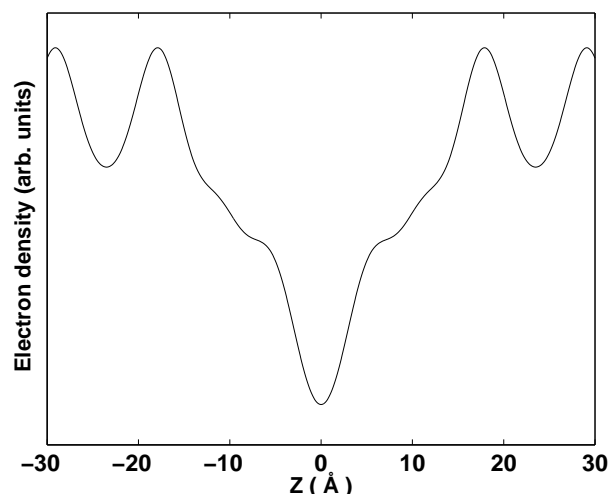


Figure 4.11: Transbilayer electron density profile of DLPE-cholesterol mixture ( $X_c = 30$  mol%,  $T = 6^\circ\text{C}$ ,  $\text{RH} = 98\%$ ). Peaks near  $\pm 20 \text{ \AA}$  and the trough at the center correspond to the head groups and terminal methyl groups of the hydrocarbon chains, respectively. Shoulder near  $\pm 10 \text{ \AA}$  are due to the presence of cholesterol.

parameters obtained from the best fit are given in tables 4.2 and 4.3, respectively. Phases obtained from the different models are the same for the stronger reflections, but phases of some of the weak reflections do change with the model and also with the starting values of the model parameters. However, changes in the phases of the weak reflections do not make any significant change in the electron density profile.

Table 4.2: Observed structure factors ( $|F_o|$ ) and their best fit values ( $F_c$ ) obtained from the three Gaussian model for DLPE-cholesterol mixture at  $X_c = 30$  mol%.

$h$	$ F_o $	$F_c$
1	10.00	-10.00
2	2.99	-2.71
3	0.42	1.06
4	3.68	-2.82
5	0.45	1.45
6	0.83	-0.32
7	0.49	-0.23
8	0.39	0.26

Table 4.3: Values of the model parameters obtained from the best fit for a DLPE-cholesterol mixture in the  $l_o$  phase ( $X_c = 30$  mol%,  $T = 6^\circ\text{C}$ ).  $x_h$  is the distance of the peak corresponding to the head group from the center of the bilayer.  $\sigma_h$  and  $\sigma_m$  are the widths of the Gaussians corresponding to the head group and the terminal methyl group, respectively.  $\rho_H$  and  $\rho_M$  are the amplitude of the Gaussians corresponding to head group and terminal methyl group, respectively.  $\Sigma$  is the function to be minimized in the fitting routine, defined in chapter 2.

$x_h$	$\sigma_h$	$\sigma_m$	$\frac{2\rho_H}{\rho_M}$	$\Sigma$
18.0	2.28	4.90	1.57	2.6

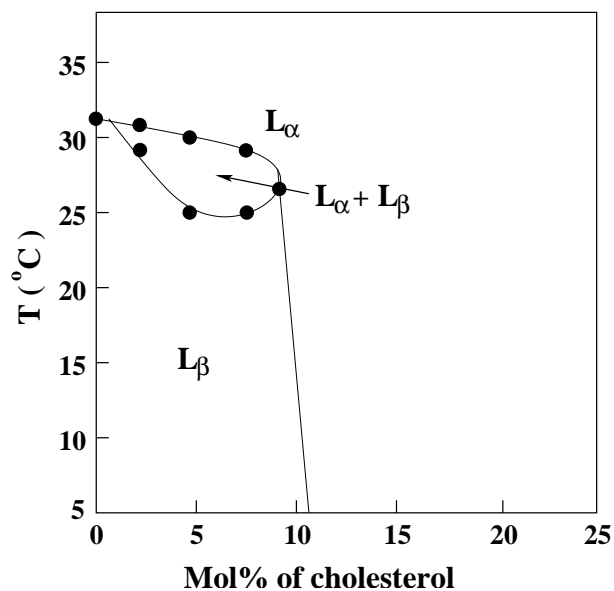


Figure 4.12: Partial phase diagram of DLPE–cholesterol mixtures at 98% RH, determined from the diffraction data collected on cooling.

## 4.5 Discussion

The phase diagram of DLPE-cholesterol mixtures obtained from the present study (Fig. 4.12) is similar to that found in POPE-cholesterol mixtures [11]. As can be seen from the phase diagram,  $T_m$  of DLPE-cholesterol mixtures decreases with increasing  $X_c$  up to 10 mol%, in agreement with earlier studies on similar systems [2, 3]. In earlier studies [2, 3, 7], the  $L_c$  phase was observed only at  $X_c > 30$  mol%. However, we have found this highly ordered phase at all cholesterol concentration before heating the sample to high temperatures. This difference could be due to the use of DLPE with shorter chains in our experiments. The lower RH (98%) used in the present experiments may also favour the formation of the highly ordered phase at lower  $X_c$ . The diffraction pattern of this phase is very similar to that of a highly ordered phase formed in pure DLPE (see Figs. 4.4 and 4.5). The formation of the highly ordered phase in PE-cholesterol mixtures, which is not easily observed in PC-cholesterol mixtures, could be the consequence of a lower miscibility of cholesterol in PE membranes. As PEs can form intermolecular hydrogen bonds among themselves, the interaction among PE molecules might be favourable over PE-cholesterol interaction, resulting in the low miscibility of cholesterol. However, at higher temperatures (above  $T_m$ ), PE-cholesterol interaction can dominate over the intermolecular hydrogen bond formation between PE molecules, leading to a high miscibility of cholesterol. We have not further analyzed these diffraction patterns to determine the structure of the highly ordered phase. It transforms into the  $L_\alpha$  phase at higher temperature, typically 45°C. This phase does not reappear on cooling which is in agreement with the earlier report by McMullen et al. [2]. The formation of a highly ordered phase was also seen in DPPC-cholesterol mixtures at  $X_c > 50$  on initial heating of the samples.

As discussed in chapter 3, dipalmitoyl phosphatidylcholine (DPPC) and dimyristoyl phosphatidylcholine (DMPC) exhibit the ripple ( $P_{\beta'}$ ) phase, characterized by a periodic height modulation of the bilayers, in between the  $L_\alpha$  and  $L_{\beta'}$  phases at high hydration. This phase is absent in PEs, and  $L_\alpha$  transforms directly into  $L_\beta$  on cooling. This difference in the

phase behaviour is believed to arise from the existence of a non-zero chain tilt in the gel phase of PCs. It is interesting that DLPE–cholesterol mixtures do not exhibit the  $P_\beta$  phase found in DPPC–cholesterol and DMPC–cholesterol mixtures. This difference again may be due to non-zero chain tilt of PC bilayer in the gel phase. It is a well established fact the  $P_\beta$  phase occurs only in lipids that exhibit chain tilt in the gel phase. Our results on DLPE–cholesterol mixtures suggest that the formation of  $P_\beta$  phase is also related to the chain tilt in the gel phase, although there seems to be no average chain tilt in this phase.

The coexistence of two phases observed in PC–cholesterol mixtures at intermediate values of  $X_c$  below  $T_m$ , discussed in the previous chapter, was also seen in DLPE–cholesterol mixtures. But there is an important difference in the nature of these two phases in PC– and PE–cholesterol mixtures. In PC–cholesterol mixtures, These two phases are the modulated ( $P_\beta$ ) and gel phases, whereas in the DLPE– cholesterol mixtures they are the fluid and gel phases. The coexistence of  $L_\alpha$  and  $L_\beta$  phases has also been reported in earlier studies of dielaidoyl phosphatidylethanolamine (DEPE)–cholesterol mixtures between 10-20 mol% of cholesterol [3]. The observed thermograms at intermediate cholesterol concentrations (5-20 mol%) seem to consist of two components, one broad and another sharp and these observations were interpreted as the coexistence of cholesterol–rich and cholesterol–poor phases. Our experimental results on DLPE–cholesterol mixtures show the coexistence at temperatures ranging from 25 to 30°C, below which we have the gel phase as indicated by a sharp wide angle reflection. In the coexistence region, partitioning of cholesterol into the two phases was not determined. The proposed experimental phase diagram based on NMR and IR spectroscopy shows the  $L_\beta$  phase coexisting with the  $l_o$  phase for  $\sim 10 < X_c < \sim 30$ , at temperatures below  $T_m$  (Fig. 4.2). At these compositions there was no gel phase detected at lower temperatures. However, our experimental results on DLPE–cholesterol mixtures show only a narrow coexistence region between  $L_\alpha$  and  $L_\beta$  phases below  $T_m$  for  $2.5 < X_c < 10$  (Fig. 4.12). This difference in the proposed phase behaviour could be due to the fact that spectroscopic techniques used in ref. [11] are sensitive to microscopic phase separation, whereas diffraction technique used here are not. Another possibility is a difference in the

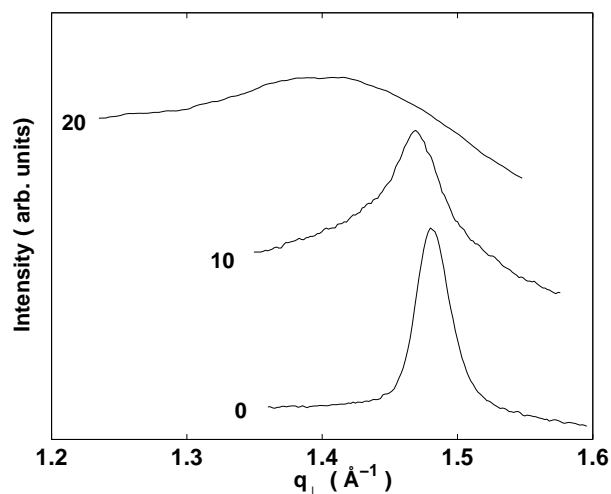


Figure 4.13: Wide angle reflections of DLPE bilayers at different cholesterol concentrations indicated by the labels on the curves ( $T = 20^{\circ}\text{C}$ ,  $\text{RH} = 98\%$ ).

phase behaviour of binary mixtures of cholesterol with POPE and DLPE, due to the presence of an unsaturated hydrocarbon chain in POPE. It is interesting to note that the  $L_{\beta}$  phase can accommodate about 10 mol% of cholesterol, whereas the  $L_{\beta'}$  phase of DPPC and DMPC can incorporate only about 2 mol% of cholesterol. This difference might be related to the fact that in the  $L_{\beta'}$  phase of PCs the hydrocarbon chains have a tilt of  $\sim 30^{\circ}$  with respect to bilayer normal.

The electron density profile of the  $l_o$  phase shows a shoulder at  $\sim \pm 10 \text{ \AA}$  due to cholesterol. The secondary maxima due to cholesterol in DPPC–cholesterol mixtures, described in previous chapter, is more prominent than that in DLPE–cholesterol mixtures although it occurs at similar distances from the bilayer center in the two cases. The less prominent cholesterol shoulder in the electron density of the DLPE–cholesterol mixtures, compared to DPPC–cholesterol mixtures, might be the consequence of almost equal lengths of DLPE and cholesterol molecules [15]. The bilayer thickness calculated from the profile is  $\sim 35 \text{ \AA}$ , in agreement with earlier results on DLPC–cholesterol mixtures at similar  $X_c$  [15].

The profiles of wide angle reflections shown in Fig. 4.13 clearly indicate that the diffraction peak gets broadened as  $X_c$  is increased. The increase in the width of the profile with increasing  $X_c$  can be attributed to the fact that positional correlations in the gel phase de-

crease with increasing  $X_c$ . In the fluid ( $L_\alpha$ ) phase of pure DLPE and DLPE–cholesterol mixture for  $X_c < 10$  mol%, the wide angle reflections have not been observed even after a long exposure in our experimental setup. However, the diffused wide angle reflections get condensed at  $q_z = 0$  at higher  $X_c$ , indicating stretching of the chains due to cholesterol, as shown in Figs. 4.8 and 4.10. A similar trend has been observed in PC–cholesterol mixtures.

## 4.6 Conclusion

DLPE–cholesterol mixtures were studied using x-ray diffraction techniques in order to probe the influence of the head group on the phase behaviour of lipid–cholesterol mixtures.  $L_\alpha$  and  $L_\beta$  phases are found to coexist at intermediate cholesterol concentrations, in agreement with earlier studies on similar systems. However, these mixtures do not exhibit the  $P_\beta$  phase. These results suggest that the formation of the  $P_\beta$  phase is confined to lipids which have a non-zero chain tilt in the gel phase. However, studies on other lipid–cholesterol mixtures are necessary to confirm this possibility.

# Bibliography

- [1] T. P. W. McMullen and R. N. McElhaney, *Biochemistry* **36**, 4979 (1997).
- [2] T. P. W. McMullen, R.N.A.H. Lewis, and R. N. McElhaney, *Biochim. Biophys. Acta* **1416**, 119 (1999).
- [3] H. Takahashi, K. Sinoda, and I. Hatta, *Biochim. Biophys. Acta* **1289**, 209 (1996).
- [4] S. L. Keller, S. M. Gruner, and K. Gawrisch, *Biochim. Biophys. Acta* **1278**, 241 (1996).
- [5] X. Wang and P. J. Quinn, *Biochim. Biophys. Acta* **1564**, 66 (2002).
- [6] G. Büldt and J. Seelig, *Biochemistry* **19**, 6170 (1980).
- [7] D. Bach and E. Wachtel, *Biochim. Biophys. Acta* **1610**, 187 (2003).
- [8] J. Huang, J. T. Buboltz, and G. W. Feigenson, *Biochim. Biophys. Acta* **1417**, 89 (1999).
- [9] R. M. Epand and R. Bottega, *Biochemistry* **26**, 1820 (1987).
- [10] X. -M. Li, M. Ramakrishnan, H. L. Brockman, R. E. Brown, and M. J. Swamy, *Langmuir* **18**, 231 (2002).
- [11] C. Pafé and M. Lafleur, *Biophys. J.* **74**, 899 (1998).
- [12] M. R. Vist and J. H. Davis, *Biochemistry* **29**, 451 (1990).
- [13] M. Aridor and W. E. Balch, *Trends Cell Biol.* **6**, 315 (1996).
- [14] R. Koynova and M. Caffrey, *Chem. Phys. Lipids* **69**, 1 (1994).
- [15] T. J. McIntosh, *Biochim. Biophys. Acta* **513**, 43 (1978).